This is a preprint, the final version is subject to change, of the American Mineralogist (MSA)
Cite as Authors (Year) Title. American Mineralogist, in press.
DOI: https://doi.org/10.2138/am-2020-7133

Revision #1

Smamite, $Ca_2Sb(OH)_4[H(AsO_4)_2]\cdot 6H_2O$, a new mineral and a possible sink for Sb during weathering of fahlore

JAKUB PLÁŠIL[1§], ANTHONY R. KAMPF[2], NICOLAS MEISSER[3], CÉDRIC LHEUR[4], THIERRY BRUNSPERGER[5] AND RADEK ŠKODA[6]

[1] Institute of Physics ASCR, v.v.i., Na Slovance 1999/2, 18221 Prague 8, Czech Republic

[2] Mineral Sciences Department, Natural History Museum of Los Angeles County, 900 Exposition Boulevard, Los Angeles, CA 90007, USA

[3] Musée cantonal de géologie, Université de Lausanne, Anthropole, Dorigny, CH-1015 Lausanne, Switzerland

[4] 1 rue du St. Laurent, 54280 Seichamps, France

[5] 22 route de Wintzenheim, 68000 Colmar, France

[6] Department of Geological Sciences, Faculty of Science, Masaryk University, Kotlářská 2, 611 37, Brno, Czech Republic

ABSTRACT

Smamite, $Ca_2Sb(OH)_4[H(AsO_4)_2]\cdot 6H_2O$, is a new mineral species from the Giftgrube mine, Rauenthal, Sainte-Marie-Aux-Mines ore-district, Haut-Rhin department, France. It is a supergene mineral found in quartz-carbonate gangue with disseminated to massive tennantite-tetrahedrite series minerals, native arsenic, Ni-Co arsenides and supergene minerals picropharmacolite, fluckite and pharmacolite. Smamite occurs as lenticular crystals growing in aggregates up to 0.5 mm across. The new mineral is whitish to colorless, transparent with vitreous luster and white streak; non-fluorescent under UV radiation. The Mohs hardness is ~3½ ; the tenacity is brittle, the fracture is curved, and there is no apparent cleavage. The measured density is 2.72(3) $g\cdot cm^{-3}$; the calculated density is 2.709 $g\cdot cm^{-3}$ for the ideal formula. The mineral is insoluble in H_2O and

§ Email: plasil@fzu.cz

quickly soluble in dilute (10 %) HCl at room temperature. Optically, smamite is biaxial (–), α = 1.556(1), β = 1.581(1), γ = 1.588(1) (white light). The 2*V* (meas.) = 54(1)°; 2*V* (calc.) = 55.1°. The dispersion is weak, *r* > *v*. Smamite is non-pleochroic. Electron microprobe analyses provided the empirical formula $Ca_{2.03}Sb_{0.97}(OH)_4[H_{1.10}(As_{1.99}Si_{0.01}O_4)_2]\cdot 6H_2O$. Smamite is triclinic, *P*–1, *a* = 5.8207(4), *b* = 8.0959(6), *c* = 8.21296(6) Å, α = 95.8343(7)°, β = 110.762(8)°, γ = 104.012(7)°, *V* = 402.57(5) Å^3 and *Z* = 1. The structure (R_{obs} = 0.027 for 1518 $I > 3\sigma I$ reflections) is based upon $\{Ca_2(H_2O)_6Sb(OH)_4[H(AsO_4)_2]\}$ infinite chains consisting of edge-sharing dimers of $Ca(H_2O)_3O_2(OH)_2$ polyhedra that share edges with $Sb(OH)_4O_2$ octahedra; adjacent chains are linked by H-bonds, including one strong, symmetrical H-bond with an O–H bond-length of ~1.23 Å. The name "smamite" is based on the acronym of the Sainte-Marie-aux-Mines district.

Keywords: smamite; new mineral species; arsenate; crystal structure; weathering; fahlore; Sainte-Marie-aux-Mines.

INTRODUCTION

Oxidative weathering of base-metal ore deposits containing complex sulfides and sulfosalts minerals leads potentially to a release of significant amounts of heavy metals and metalloids, especially of As, Pb, Bi or Sb into the environment. Supergene minerals formed during weathering in oxidation zones of these deposits then serve as a temporary or final sink for toxic elements otherwise released into the groundwater. Therefore, an exact knowledge of the supergene mineralogy of a particular deposit is of great importance as it can be used to assess and predict the behavior and mobility of elements during weathering, both natural or anthropogenically induced (e.g., Borčinová-Radková et al. 2017; Keim et al. 2018; Majzlan et al.

2018; Dordević et al. 2019, and references therein). Smamite, a new hydrated arsenate mineral containing Sb(V) as an essential component, is formed *via* oxidative weathering of a complex hypogene mineral association at Sainte-Marie-Aux-Mines district (France) in the conditions of the old mine workings. Although it is currently known only from a few specimens, it is likely to be much more common, having been overlooked due to its inconspicuous appearance. Therefore, it may prove to be another important sink for antimony in supergene weathering assemblages.

The new mineral is based on the acronym "SMAM" for the type locality, the famous **S**ainte-**Ma**rie-**A**ux-**Mi**nes polymetallic mining district, in Haut-Rhin department, France. The mining district of Sainte-Marie is known both for its long-lasting mining activities in the past and for its interesting mineralogy. It has yielded nine new arsenate mineral species: ferrarisite (Bari et al. 1980a), fluckite (Bari et al. 1980b), mcnearite (Sarp et al. 1981), phaunouxite (Bari et al., 1982), rauenthalite (Pierrot 1964), sainfeldite (Pierrot 1964), villyaellenite (Sarp 1984), weilite (Herpin and Pierrot 1963), and giftgrubeite (Meisser et al. 2019). The new mineral and name were approved by the Commission on New Minerals, Nomenclature and Classification of the International Mineralogical Association (IMA 2019-001). One holotype and two cotype specimens are deposited in the Mineralogical Collection of the Musée cantonal de géologie, University of Lausanne, Anthropole, Dorigny, CH-1015 Lausanne, Switzerland, the catalogue number MGL n° 093481, 093482 and 093483 respectively. One cotype specimen is deposited in the mineral collections of the Natural History Museum of Los Angeles County, under catalogue number 67169.

OCCURRENCE

Smamite was found in the Giftgrube mine, which exploits the famous St. Jacques vein

rich in arsenic, in Rauenthal, Sainte-Marie-Aux-Mines, Haut-Rhin department, Grand Est, France. It is a supergene mineral resulting from the weathering of primary As-mineralization (mainly consisting of native arsenic, tennantite-tetrahedrite, arsenides of Co and Ni, löllingite and chalcopyrite) in the old mine workings. The supergene minerals associated with smamite include picropharmacolite, fluckite, pharmacolite, quartz and carbonates (calcite and dolomite). The Giftgrube mine was apparently first mined in the 16th century and some galleries were reopened later, especially during the 18th century. The Giftgrube mine is also the type locality for the recently discovered mineral giftgrubeite (Meisser et al. 2019).

PHYSICAL AND OPTICAL PROPERTIES

Crystals of smamite are lenticular in shape; forming aggregates up to about 0.5 mm in size (Figs. 1 and 2). The mineral is white to colorless, transparent with vitreous luster and white streak. Smamite is nonfluorescent in long- or short-wave ultraviolet light. It has a Mohs hardness of about 3½, brittle tenacity, curved fracture, and no apparent cleavage. The density measured by flotation in a mixture of diiodomethane/1-chloronaphtalene (23.5°C; n = 3) is 2.72(3) g·cm^{-3}. The calculated density is 2.690 g·cm^{-3} for the empirical formula and 2.709 g·cm^{-3} for the ideal formula. The mineral is insoluble in H_2O and quickly soluble in dilute (10 %) HCl at room temperature. After H_2O dilution of the HCl solution, a white Sb-oxychloride precipitate slowly forms.

Smamite is optically biaxial (–) with indices of refraction α = 1.556(1), β = 1.581(1), γ = 1.588(1) measured in white light. The 2V measured using extinction data analyzed with EXCALIBRW (Gunter et al. 2004) is 54(1)°; the calculated 2V is 55.1°. The dispersion is weak, r > v. The optical orientation was not determined. Smamite is non-pleochroic. The Gladstone–Dale

compatibility, $1 - (K_P/K_C)$, (Mandarino 2007) is -0.014 (superior) using the empirical formula.

RAMAN SPECTROSCOPY

Raman spectroscopy was conducted on a Jobin-Yvon Labram HR Evolution system, using a 600 lines/mm grating and a He–Ne 633 nm laser with a beam power of 10 mW at the sample surface. The spectrum was collected from 4000 to 100 cm^{-1} (Fig. 3). Band fitting was done after appropriate background correction, assuming combined Lorentzian-Gaussian band shapes using the Voigt function (*PeakFit*; Jandel Scientific Software).

The Raman spectrum is dominated by the stretching vibrations of AsO_4 tetrahedra. The broad, but resolved band (~3500–3000 cm^{-1}) consisting of several overlapping bands (3510, 3433, 3384, 3521, 3148 cm^{-1}) corresponds to O–H stretching vibrations. According to the correlation given by Libowitzky (1999), these vibrations correspond to H-bonds (H···*Acceptor*) in the range 2.1–1.7 Å. These values are in line with those obtained from the structure determination. There are no bands that can be reliably assigned to the ν_2 (δ) H–O–H as it is overlapped by strong fluorescence. The overlapping composite band of medium intensity composed of bands at 892, 870, 850 and 826 cm^{-1} is attributed to ν_3 antisymmetric and the ν_1 symmetric As–O vibrations of the As-tetrahedra. A shoulder at 788 cm^{-1} is most probably related to the out-of-plane bending vibration of the Sb–O-H. A sharp band of highest intensity, at 642 cm^{-1}, is probably related to the antisymmetric stretching vibration of the O–Sb–O–As–O linkage in $[Sb(OH)_4O_2(AsO_4)]$ fragments. Bands of low intensity at 585, 547 and 510 cm^{-1} are overlapping Sb–O stretching vibrations of $Sb(OH)_4O_2$ and ν_4 (δ) O–As–O tetrahedra. Bands of low intensity at 418, 401, 372, 339, 289, 254 cm^{-1} and two bands with high intensity at 234 and 212 cm^{-1} are related to ν_2 (δ) O–As–O bending vibrations and various bending H-O–Sb and H-

120 O–As vibrations. The bands at the lowest energies are due to phonons.

121

122 ## CHEMICAL ANALYSIS

123 Smamite was analyzed in a polished section with a Cameca SX-100 electron microprobe
124 operating in WDS mode using 15 kV accelerating voltage, 4 nA beam current and a beam
125 diameter of 10 μm. Raw X-ray intensities were corrected for matrix effects with a $\phi\rho(z)$
126 algorithm of X-PHI routine (Merlet 1994). Because insufficient material was available for a
127 direct determination of H_2O, the amount of water was calculated on the basis of stoichiometry (5
128 total cations *pfu*, 18 O *apfu* and charge balance) as indicated by the structure. Analytical data are
129 given in Table 1. The empirical formula is $Ca_{2.03}Sb_{0.97}(OH)_4[H_{1.10}(As_{1.99}Si_{0.01}O_4)_2]\cdot 6H_2O$. The
130 ideal formula is $Ca_2Sb(OH)_4[H(AsO_4)_2]\cdot 6H_2O$, which requires CaO 17.07, Sb_2O_5 24.63, As_2O_5
131 34.99, H_2O 23.31, total 100 wt%.

132

133 ## X-RAY CRYSTALLOGRAPHY AND STRUCTURE DETERMINATION

134 Both powder and single-crystal X-ray studies were carried out using a Rigaku R-Axis
135 Rapid II curved imaging plate microdiffractometer with monochromatized Mo*K*α radiation. For
136 the powder study, a Gandolfi-like motion geometry on the φ and ω axes was used to randomize
137 the sample. Observed *d* values and intensities were derived by profile fitting using JADE 2010
138 software. Data are given in Table 2. Triclinic unit-cell parameters refined from the powder data
139 using JADE 2010 with whole pattern fitting are $a = 6.822(5)$, $b = 8.094(5)$, $c = 8.218(5)$ Å, $\alpha =$
140 $95.80(2)°$, $\beta = 110.77(2)°$, $\gamma = 104.94(2)°$, and $V = 403.0(2)$ Å^3.

141 A small 90 × 90 × 40 μm fragment of adequate crystal quality was chosen for the data
142 collection; details are given in Table 3. The Rigaku CrystalClear software package was used for

143 processing the structure data, including the application of an empirical absorption correction
144 using the multi-scan method with ABSCOR (Higashi, 2001). The structure was solved using
145 SHELXT program (Sheldrick 2015) and was refined by the least-squares algorithm in Jana2006
146 (Petříček et al. 2014) based on F^2. Some of the O atoms and, in particular, the H atoms were
147 located from the difference Fourier maps. The H atoms were refined with soft constraints on the
148 O–H distances and U_{iso} of the H atoms was set at 1.2 times that of the corresponding donor O
149 atom. The refinement converged smoothly to $R = 0.0274$ and $wR = 0.0679$ for 1518 unique
150 observed reflections (GOF = 1.68) (Table 3). Atom coordinates and displacement parameters are
151 listed in Tables 4 and 5; selected interatomic distances and a bond-valence analysis are provided
152 in Tables 6 and 7, respectively.
153

154 **DESCRIPTION OF THE STRUCTURE**

155 Smamite has a unique structure (Figs. 4a, b), with several remarkable features (see
156 below). The structure contains one Sb, one Ca, one As, nine H and nine O atoms in the
157 asymmetric unit (all atoms occupying 2*i* sites, except of Sb and H5, which occupy 1*g* and 1*d*
158 sites, respectively). The Sb site is coordinated as a regular octahedron, in which the four
159 equatorial vertices are OH groups (two symmetrically related sites OH2 and OH3) and the two
160 apical apices (related by an inversion center) are O atoms (O1 and O1'). The occupancy of the Sb
161 site refined to less than unity. The Ca site is 7–coordinated by two O atoms, two OH groups and
162 three H_2O groups (Table 6). The As^{5+} is coordinated as a regular tetrahedron by three O atoms,
163 while the fourth vertex of the tetrahedron is protonated (linking the H5 atom, see below). The
164 structure is based upon $\{Ca_2(H_2O)_6Sb(OH)_4[H(AsO_4)_2]\}$ infinite chains running approximately
165 parallel to (-111). These chains result from edge-sharing dimers of $Ca(H_2O)_3O_2(OH)_2$ polyhedra

that in turn share edges with $Sb(OH)_4O_2$ octahedra. The chain is decorated by AsO_4 tetrahedra pointing up and down along the length of the chain (Fig. 5). Adjacent chains are linked by H-bonds. There is a particularly interesting short, symmetrical H-bond, O5–H5–O5' (Fig. 3a) with an O–H bond-length of ~1.23 Å. Such strong, symmetrical H-bond has been already reported in structures of arsenate minerals and compounds (Ferraris et al. 1971, 1972; Ondruš et al. 2013). These H-bonds has an O-H bond-lengths of ~1.22 Å. Considering the refined site occupancies and the bond-valence sums, the structural formula for smamite is $Ca_2(H_2{}^{[3]}O)_4(H_2{}^{[4]}O)_2Sb_{0.94}(OH)_4[H(AsO_4)_2]$, $Z = 1$. We note that this formula has a net charge of -0.3 due to a 0.06 deficiency in the Sb^{5+} occupancy. However, we cannot be certain that the deficit in Sb occupancy is real or is an artefact perhaps caused by an inadequate absorption correction. If it is real, it could be compensated by additional protonation of the arsenate group.

There is no mineral structurally similar to smamite. The presence of both Sb^{5+} and As^{5+} suggests strongly oxidizing conditions of formation. Richelsdorfite (Süsse and Tillman 1987) and joelbruggerite (Mills et al. 2009) also contain both Sb^{5+} and As^{5+}, but their structures are completely different than that of smamite. Another recently approved Ca, Sb and As containing mineral, prachařite, $CaSb_2{}^{5+}(As_2{}^{3+}O_5)_2O_2 \cdot 10H_2O$ (Kolitsch et al. 2018), contains trivalent arsenic and a structure that is quite distinct.

IMPLICATIONS

The new mineral smamite was formed *via* supergene oxidative weathering of a rather complex mineral assemblage including fahlore (minerals of the tetrahedrite-tennantite series), Ni-As minerals and native arsenic. The evolution of the supergene association is likely to have involved several steps. The first step is probably the oxidation of massive or disseminated native

arsenic and the formation of As_2O_3, which is thermodynamically favored (Majzlan et al. 2014). The As_2O_3 oxidizes in contact with humid air or descending (meteoric) water, yielding strongly acidic solutions containing As^{5+} as various hydrogenarsenate anions, e.g. $(H_2AsO_4)^-$ and $(HAsO_4)^{2-}$ (c.f., Majzlan et al. 2014). Such solutions then attack gangue carbonates, here mostly Mn–Fe bearing calcite and dolomite, and partly oxidized tennantite-tetrahedrite (fahlore), which shifts the pH to more alkaline (*c.f.*, model 3Aa of Markl et al. 2014), and this results in the deposition of smamite (as the only Ca–bearing antimonate-arsenate), picropharmacolite (as the main Mg–bearing arsenate) and fluckite (as the main Mn–bearing arsenate).

Weathering of Sb-ores and the fate of Sb in the environment has been much less studied that of As. A few recent studies have shown that the common products of supergene weathering of primary Sb ores comprise Sb-bearing minerals of the pyrochlore group (stibiconite, roméite, and bindheimite) and tripuhyite, $Fe^{3+}Sb^{5+}O_4$, accompanied often by goethite and hydrous ferric oxide with adsorbed or incorporated Sb (Keim et al. 2018; Majzlan et al. 2018, and references therein). A recently published study on the redistribution of elements during oxidative dissolution of tetrahedrite from Piesky, Slovakia (Majzlan et al. 2018) has documented that ~10 % As and almost 50 % of Sb (from the initial 100 % in primary tetrahedrite) are lost during weathering. Likely, they are being released into water with some Sb stored in the supergene minerals camérolaite, cualstibite and tripuhyite. According to Majzlan et al. (2018), antimony is more abundant than arsenic in the aqueous fluids and all contaminated water samples are supersaturated with respect to tripuhyite. In the system, which is overall poor in arsenic overall, antimony associates temporarily with Ca or Al, but is slowly converted to the "ultimate sink", which is tripuhyite. One can speculate that, in the As-rich environment, which is also rich in Sb, smamite and other possible new mineral phases in the system *Me*–Sb^{5+}–AsO_4–H_2O may serve as

sinks for Sb, due to their low solubility in aqueous solutions with circumneutral pH (by analogy with smamite).

ACKNOWLEDGEMENTS

William Perraud is acknowledged for providing us with the microphotography of smamite. Comments by Juraj Majzlan and an anonymous reviewer as well as the structure editor helped in improving the manuscript.. This study was funded, in part, by the John Jago Trelawney Endowment to the Mineral Sciences Department of the Natural History Museum of Los Angeles County and by the Czech Science Foundation (GACR 17-09161S) to JP.

REFERENCES

Bari, H., Permingeat, F., Pierrot, R., and Walenta, K. (1980a) La ferrarisite, $Ca_5H_2(AsO_4)_4 \cdot 9H_2O$, une nouvelle espèce minérale isomorphe de la guérinite. Bulletin de la Societé Française de Minéral et de Cristallographie, 103, 533–540.

Bari, H., Cesbron, F., Permingeat, F., and Pillard, F. (1980b) La fluckite, arséniate hydraté de calcium et manganèse, $CaMnH_2(AsO_4)_2 \cdot 2H_2O$, une nouvelle espèce minérale. Bulletin de la Societé Française de Minéral et de Cristallographie, 103, 122–128.

Bari, H., Catti, M., Ferraris, G., Ivaldi, G., and Permingeat, F. (1982) Phaunouxite, $Ca_3(AsO_4)_2 \cdot 11H_2O$, a new mineral strictly associated with rauenthalite. Bulletin de la Societé Française de Minéral et de Cristallographie, 105, 327–332.

Borčinová Radková, A., Jamieson, H., Lalinská-Voleková, B., Majzlan, J., Števko, M., and Chovan, M. (2017) Mineralogical controls on antimony and arsenic mobility during tetrahedrite-tennantite weathering at historic mine sites Špania Dolina-Piesky and Ľubietova-Svatodušná, Slovakia. American Mineralogist, 102, 1091–1100.

Brown, I. D. (2002) The Chemical Bond in Inorganic Chemistry: The Bond Valence Model; Oxford University Press: Oxford, 2002.

Đorđević, T., Kolitsch, U., Serafimovski, T., Tasev, G., Tepe, N., Stöger-Pollach, M., Hofmann, T., and Boev, B. (2019) Mineralogy and Weathering of Realgar-Rich Tailings At a Former As-Sb-Cr Mine At Lojane, North Macedonia. Canadian Mineralogist, 57, 403–423.

Ferraris, G., Jones, D.W., and Yerkess, J. (1971) Symmetrical hydrogen bonds in the crystal structure of calcium bis(dihydrogen arsenate): a neutron-diffraction study. Journal of the Chemical Society. D23, 1566–1567.

Ferraris, G., Jones, D.W., and Yerkess, J. (1972) A neutron diffraction study of the crystal structure of calcium bis(dihydrogen arsenate), Ca(H2AsO4)2. Acta Crystallographica, B28, 2430–2437.

Gagné, O.C., and Hawthorne, F.C (2015) Comprehensive derivation of bond-valence parameters for ion pairs involving oxygen. Acta Crystallographica, B71, 562–578.

Gunter, M.E., Bandli, B.R., Bloss, F.D., Evans, S.H., Su, S.C., and Weaver, R. (2004) Results from a McCrone spindle stage short course, a new version of EXCALIBR, and how to build a spindle stage. The Microscope, 52, 23-39.

Herpin, P., and Pierrot, R. (1963) La weilite, $CaH(AsO_4)$, un nouvel arséniate de calcium isomorphe de la monétite. Bulletin de la Societé Française de Minéral et de Cristallographie, 86, 368–372.

Higashi, T. (2001) ABSCOR. Rigaku Corporation, Tokyo.

Keim, M.F., Staude, M., Marquardt, K., Bachmann, K., Opitz, J., and Markl, G. (2018) Weathering of Bi-tennantite. Chemical Geology, 499, 1–25.

Kolitsch, U., Sejkora, J., Topa, D., Kampf, A.R., Plášil, J., Rieck, B., and Fabritz, K.H. (2018) Prachařite, IMA 2018-081. CNMNC Newsletter No. 46, December 2018, page 1183; European Journal of Mineralogy, 30, 1181–1189.

Larsen, E.S. (1921) The microscopic determination of the nonopaque minerals. U.S. Geological Survey, Bulletin 679.

Majzlan, J., Plášil, J., Škoda, R., Gescher, J., Kögler, P., Rusznyak, A., Küsel, K., Neu, T.R., Mangold, S., and Rothe, J. (2014) Arsenic-rich acid mine water with extreme arsenic concentration: mineralogy, geochemistry, microbiology, and environmental implications. Environmental Science & Technology, 48, 13685–13693.

Majzlan, J., Kiefer, S., Hermann, J., Števko, M., Sejkora, J., Chovan, M., Láncosz, T., Lazarov, M., Gerdes, A., Langenhorst, F., Borčinová-Radková, A., Jamieson, H., and Milovský, R. (2018) Synergies in elemental mobility during weathering of tetrahedrite [$(Cu,Fe,Zn)_{12}(Sb,As)_4S_{13}$]: Field observations, electron microscopy, isotopes of Cu, C, O, radiometric dating, and water geochemistry. Chemical Geology, 488, 1–20.

Mandarino, J.A. (2007) The Gladstone–Dale compatibility of minerals and its use in selecting mineral species for further study. Canadian Mineralogist, 45, 1307-1324.

Markl, G., Marks, M.A.W., Derrey, I., and Gühring, J.E. (2014) Weathering of cobalt arsenides: natural assemblages and calculated stability relations among secondary Ca–Mg–Co arsenates and carbonates. American Mineralogist, 99, 44–56.

Meisser, N., Plášil, J., Brunsperger, T., Lheur, C., Škoda, R. (2019) Giftgrubeite, $CaMn_2Ca_2(AsO_4)_2(AsO_3OH)_2{\cdot}4H_2O$, a new member of the hureaulite group from Sainte-Marie-aux-Mines, Haut-Rhin Department, Vosges, France. Journal of Geosciences, 64, 73–80.

280 Merlet C. (1994) An Accurate Computer Correction Program for Quantitative Electron Probe
281 Microanalysis, Microchimica Acta, 114/115, 363–376.
282 Mills, S.J., Kolitsch, U., Miyawaki, R., Groat, L.A., and Poirier, G. (2009) Joëlbruggerite,
283 $Pb_3Zn_3(Sb^{5+},Te^{6+})As_2O_{13}(OH,O)$, the Sb^{5+} analogue of dugganite, from the Black Pine mine,
284 Montana. American Mineralogist, 94, 1012–1017.
285 Petříček, V., Dušek, M., and Palatinus, L. (2014) Crystallographic Computing System Jana 2006:
286 general features. Zeitschrift für Kristallographie, 229, 345–352.
287 Pierrot, R. (1964) Contribution à la minéralogie des arséniates calciques et calcaromagnésiens
288 naturels. Bulletin de la Societé Française de Minéral et de Cristallographie, 87, 169–211.
289 Sarp, H. (1984) Villyaellenite, $H_2(Mn,Ca)_5(AsO_4)_4 \cdot 4H_2O$ un nouveau mineral de Sainte-Marie
290 aux-Mines (France). Schweizerische mineralogishe petrographische Mitteilungen, 64, 323–
291 328.
292 Sarp, H., Deferne, J., and Liebich, B.W. (1981) La mcnéarite, $NaCa_5H_4(AsO_4)_5 \cdot 4H_2O$, un nouvel
293 arséniate hydraté de calcium et de sodium. Schweizerische mineralogishe petrographische
294 Mitteilungen, 61, 1–6.
295 Süsse, P., and Tillmann, B. (1987) The crystal structure of the new mineral richelsdorfite,
296 $Ca_2Cu_5Sb(Cl/(OH)_6/(AsO_4)_4) \cdot 6H_2O$. Zeitschrift für Kristallographie, 179, 323–334.
297 Sheldrick, G.M. (2015) Crystal structure refinement with SHELXL. Acta Crystallographica, C71,
298 3–8.
299

300 FIGURE CAPTIONS

301 Figure 1. Lenticular crystals of smamite from Giftgrube mine, Sainte-Marie-Aux-Mines.
302 Horizontal field of view is 0.6 mm (photo W. Perraud).

303

304 Figure 2. Aggregate of smamite crystals with apparently stepped faces. SE image (photo C.
305 Lheur).

306

307 Figure 3. Raman spectrum of smamite with fitted band-components: a) in the range 1100–100
308 cm^{-1}, b) 3800–2800 cm^{-1}.

309

310 Figure 4. Packing of infinite chains in the structure of smamite viewed along **a)** [100] direction.
311 Notice the short O5–H5–O5 hydrogen bond that provides additional extra-chain linkage. **b)** In a
312 general direction, approximately parallel to the length of chains. Color scheme is same as in the
313 previous figure. Unit-cell edges are outlined in black solid lines.

314

315 Figure 5. Infinite chain found in the structure of smamite. The As-tetrahedra are in green color.

316

This is a preprint, the final version is subject to change, of the American Mineralogist (MSA)
Cite as Authors (Year) Title. American Mineralogist, in press.
DOI: https://doi.org/10.2138/am-2020-7133

This is a preprint, the final version is subject to change, of the American Mineralogist (MSA)
Cite as Authors (Year) Title. American Mineralogist, in press.
DOI: https://doi.org/10.2138/am-2020-7133

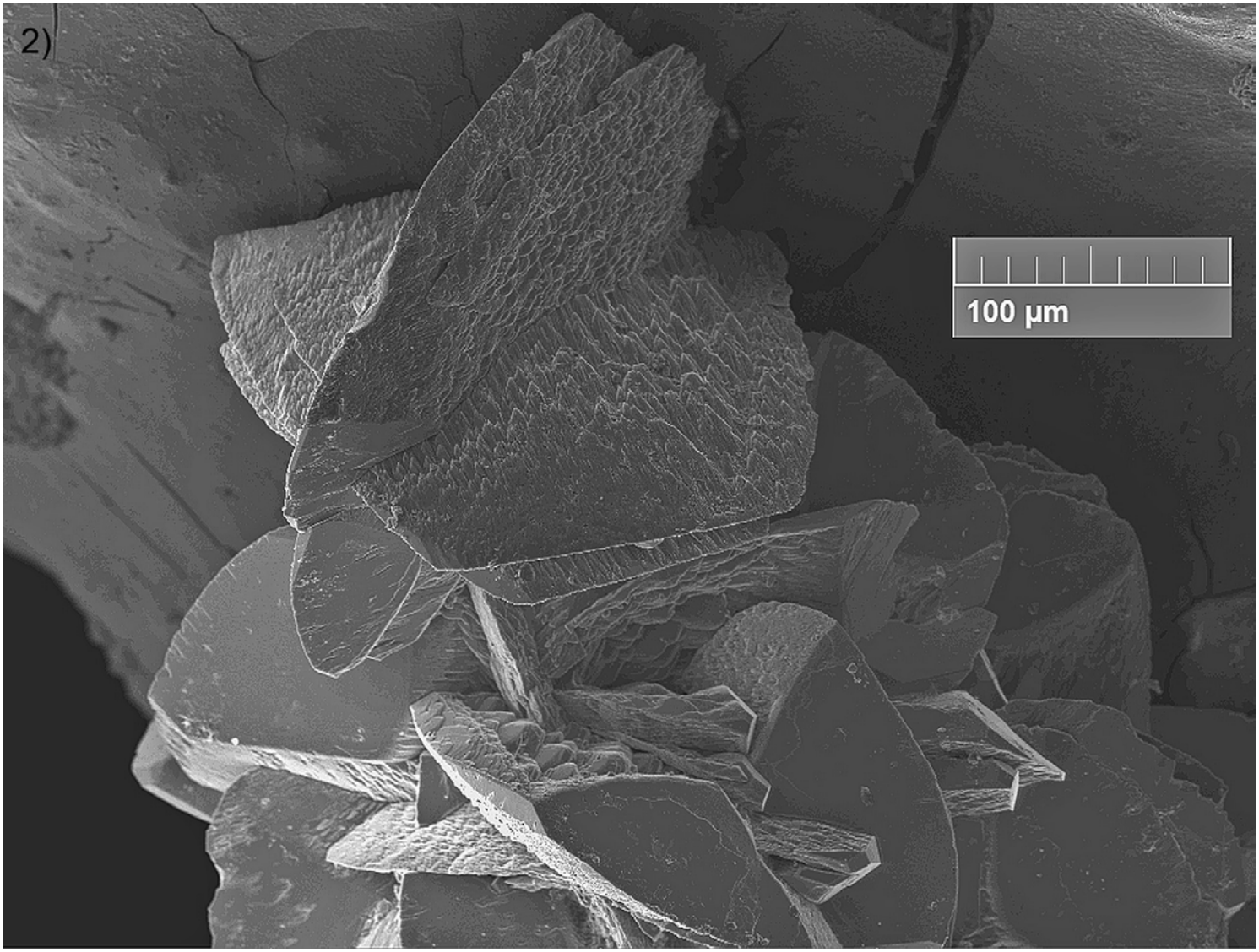

This is a preprint, the final version is subject to change, of the American Mineralogist (MSA)
Cite as Authors (Year) Title. American Mineralogist, in press.
DOI: https://doi.org/10.2138/am-2020-7133

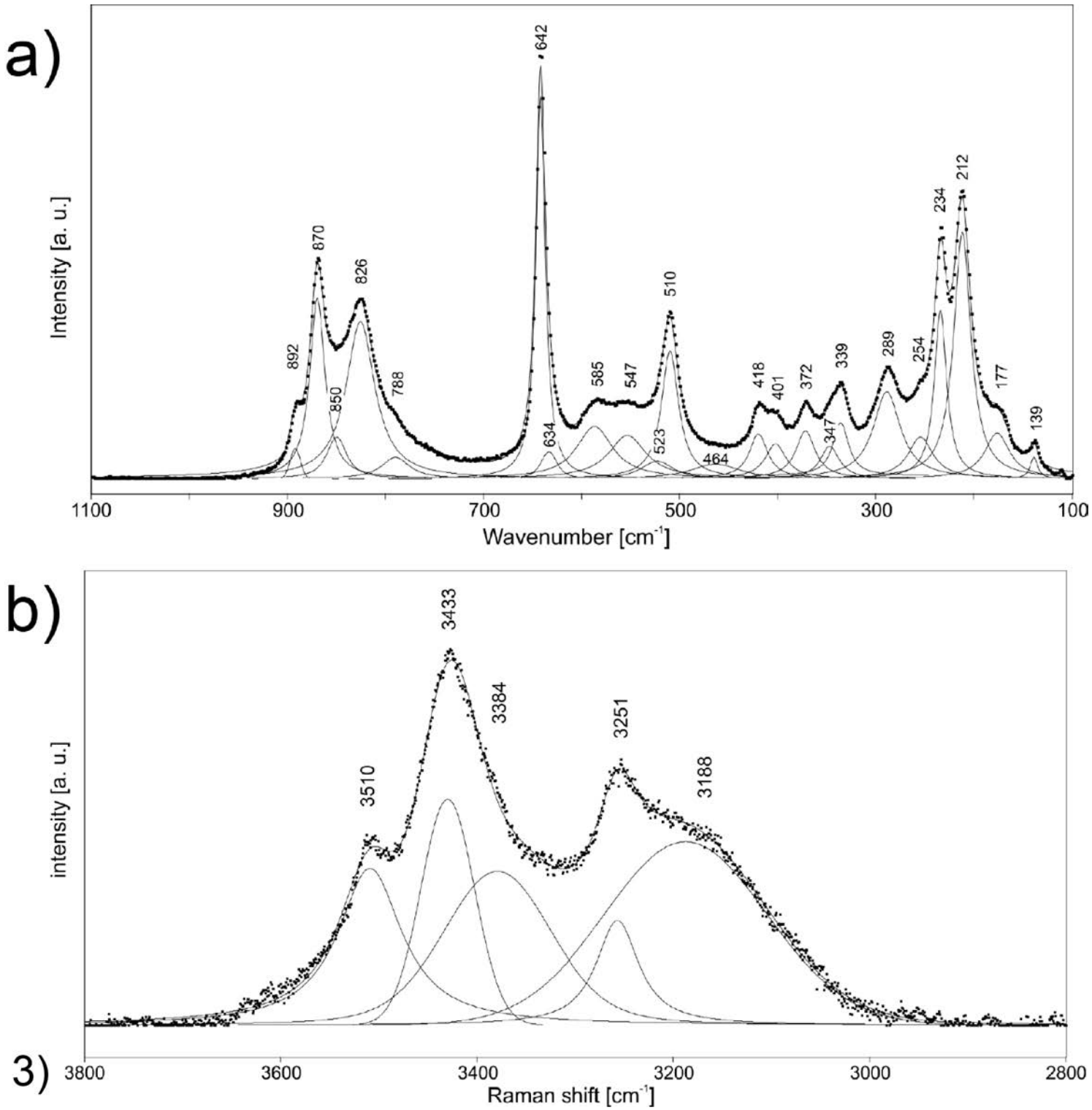

This is a preprint, the final version is subject to change, of the American Mineralogist (MSA)
Cite as Authors (Year) Title. American Mineralogist, in press.
DOI: https://doi.org/10.2138/am-2020-7133

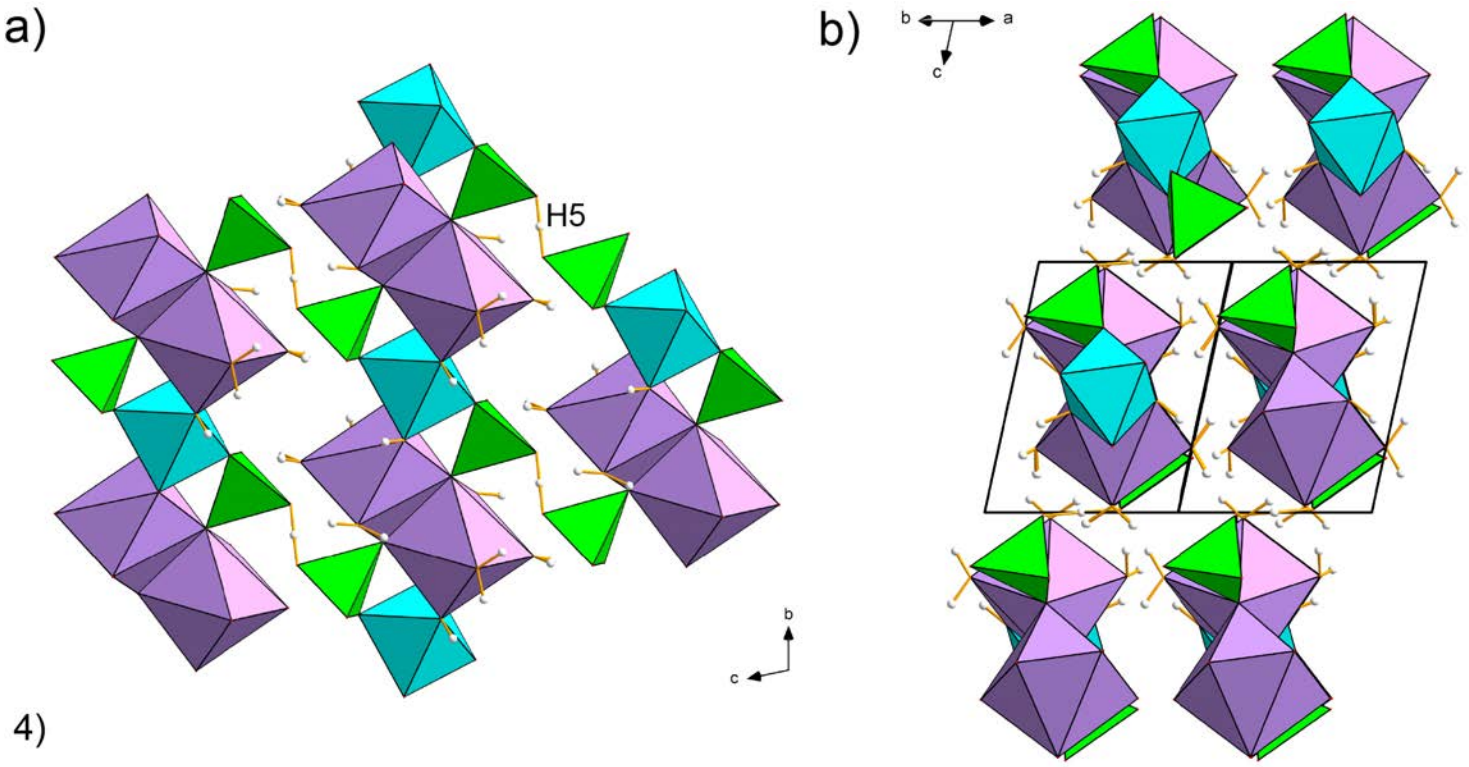

4)

This is a preprint, the final version is subject to change, of the American Mineralogist (MSA)
Cite as Authors (Year) Title. American Mineralogist, in press.
DOI: https://doi.org/10.2138/am-2020-7133

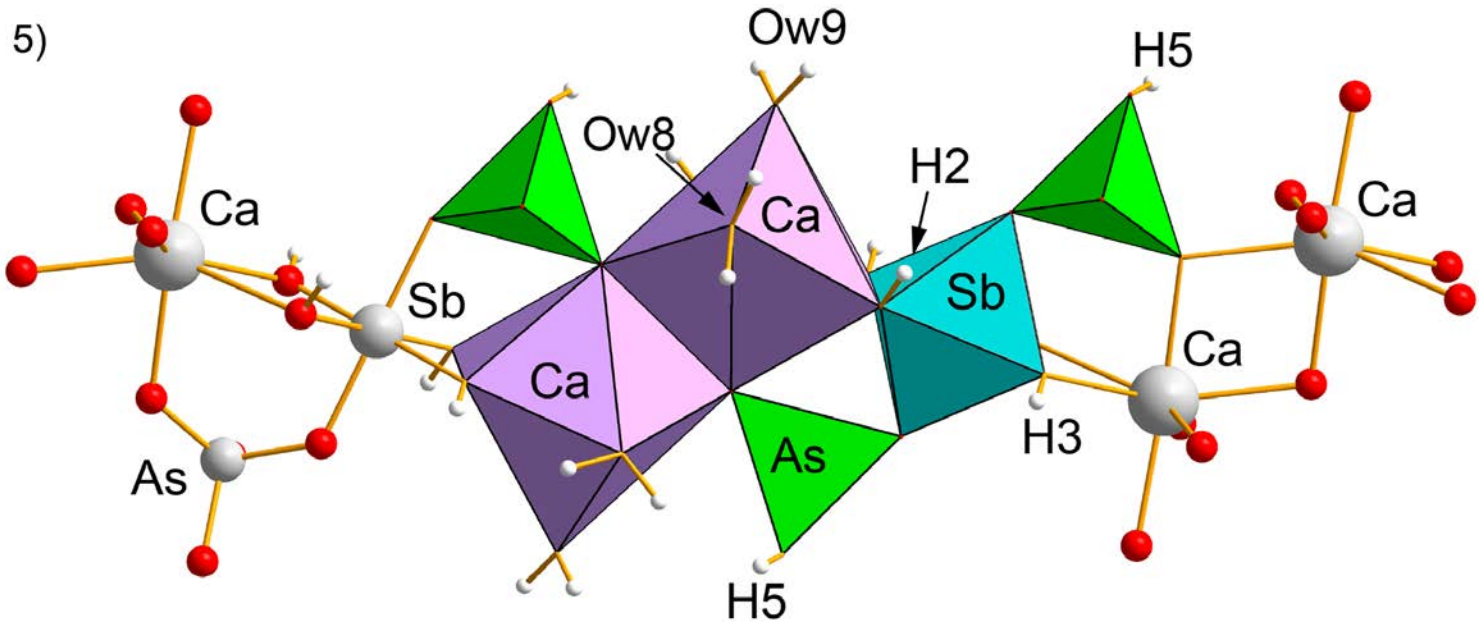

This is a preprint, the final version is subject to change, of the American Mineralogist (MSA)
Cite as Authors (Year) Title. American Mineralogist, in press.
DOI: https://doi.org/10.2138/am-2020-7133

Table 1. Analytical results for smamite [wt%].

Constituent	**Mean**	**Range**	**Stand. Dev.**	**Probe Standard**
CaO	17.34	17.07–17.72	0.30	andradite
Sb_2O_5	23.92	22.33–25.62	1.29	metallic Sb
SiO_2	0.12	0.00–0.20	0.08	sanidine
As_2O_5	34.93	33.69–36.44	1.49	lammerite
H_2O*	23.50			
Total	**99.81**			

* based on structure.

This is a preprint, the final version is subject to change, of the American Mineralogist (MSA)
Cite as Authors (Year) Title. American Mineralogist, in press.
DOI: https://doi.org/10.2138/am-2020-7133

Table 2. Powder X-ray data (d in Å) for smamite. Only calculated lines with $I \geq 2$ are listed.

I_{obs}	d_{obs}	d_{calc}	I_{calc}	hkl
41	**7.56**	7.6855	11	0 1 0
		7.5139	43	0 0 1
		6.0860	4	1 0 0
60	**6.03**	6.0318	80	0-1 1
47	**5.66**	5.6666	66	-1 1 0
100	**5.07**	5.0745	100	-1 1 1
1	4.50	4.4680	3	-1-1 1
43	**3.992**	4.0197	30	1 0 1
		3.9686	29	-1 0 2
		3.8427	7	0 2 0
		3.8029	25	-1 2 0
36	**3.783**	3.7569	6	0 0 2
		3.7498	18	0-2 1
28	3.551	3.5602	34	-1-1 2
		3.4932	6	-1 1 2
4	3.342	3.3358	6	-2 1 1
		3.1820	13	1 1 1
24	3.148	3.1663	4	0 2 1
		3.1297	20	0 1 2
		3.0641	7	-1-2 1
28	3.035	3.0430	22	2 0 0
		3.0159	16	0-2 2
		2.9386	4	-2 1 2
		2.8833	22	1 2 0
51	**2.858**	2.8626	5	1-1 2
		2.8602	28	-2 2 1
		2.8094	29	-2-1 1
31	**2.766**	2.7934	8	-1-2 2
		2.7503	32	1 0 2
		2.6888	4	-2-1 2
8	2.649	2.6433	6	-1-1 3
		2.6328	6	2-1 1
		2.5618	3	0 3 0
24	2.545	2.5447	26	1-3 1
		2.5372	3	-2 2 2
13	2.460	2.4668	8	-2 0 3
		2.4456	8	0 2 2
6	2.362	2.3821	5	1 1 2
		2.3552	5	0-3 2
		2.3235	3	-1-2 3
19	2.255	2.2848	6	0 3 1
		2.2484	16	0 1 3
		2.2180	3	1-3 2
12	2.182	2.1865	6	-3 0 1
		2.1782	16	-3 0 2
5	2.126	2.1322	6	-1 2 3
		2.1101	4	2-1 2
7	2.061	2.0673	8	-3 2 0
		2.0535	5	1-2 3
		2.0132	3	-1 4 0
13	1.9953	2.0087	4	-3 1 3
		1.9843	13	-2 0 4
		1.9214	3	0 4 0
		1.9185	5	0-1 4
		1.9038	6	-1 4 1
24	1.9010	1.9014	9	-2 4 0
		1.8889	4	2-3 2
		1.8844	4	-3-1 3
		1.8785	6	0 0 4
		1.8604	4	3-2 1
		1.8537	6	-3 3 2
21	1.8450	1.8467	5	2 2 1
		1.8421	5	1-4 2
		1.8372	4	-2-3 2
		1.8310	3	3 1 0
		1.8257	8	2-4 1
		1.7866	3	-1 3 3
		1.7475	3	-3 1 4
14	1.7442	1.7454	10	-1-4 2
		1.7434	8	-2-3 3
		1.7138	3	-1 4 2
		1.7123	4	-1 2 4
17	1.7002	1.7013	8	-4 1 2
		1.6988	4	-1-3 4
		1.6920	7	-3-2 3
		1.6575	6	1-2 4
13	1.6514	1.6532	4	1 3 2
		1.6429	3	2 0 3
		1.6337	5	3 1 1
		1.6186	7	2-3 3
16	1.6171	1.6139	5	-1 0 5
		1.6111	3	-4 0 3
		1.5910	5	2 2 2
8	1.5717	1.5784	3	-4 3 1
		1.5667	4	-3-2 4
		1.5452	3	-2 4 3
14	1.5403	1.5436	4	2-5 1
		1.5384	4	0-5 2
		1.5360	3	-1 1 5
		1.5316	4	-2-2 5
		1.5215	7	4 0 0
14	1.5141	1.5172	3	2 1 3
		1.5119	3	1 1 4
		1.5080	4	0-4 4
		1.4823	3	-3-3 1
		1.4629	5	-1-3 5
9	1.4496	1.4478	7	3-4 2
		1.4416	4	2 4 0
3	1.4303	1.4287	3	1-5 3
6	1.3950	1.3967	3	-2-4 4
		1.3889	3	4 0 1
2	1.3695	1.3641	3	-4 4 3
8	1.3329	1.3369	4	-5 2 3
		1.3281	3	-5 1 1

This is a preprint, the final version is subject to change, of the American Mineralogist (MSA)
Cite as Authors (Year) Title. American Mineralogist, in press.
DOI: https://doi.org/10.2138/am-2020-7133

Table 3. Data collection and structure refinement details for smamite.

Formula	$Ca_2(H_2O)_6Sb_{0.94}(OH)_4[H(AsO_4)_2]$
a, *b*, *c* [Å]	6.8207(4), 8.0959(6), 8.21296(6)
α, β, γ [°]	95.8343(7), 110.762(8), 104.012(7)
V [Å^3]	402.57(5)
Z	1
Space group	*P*–1
D_{calc} (g cm^{-3})	2.678
Temperature	293 K
Wavelength	Mo*K*α, 0.71073 Å
Crystal dimensions	90 × 90 × 40 μm
Collection mode	ω scans to fill an Ewald sphere
Limiting θ angles	3.35–27.44°
Limiting Miller indices	$-8<h<8$, $-10<k<10$, $-10<l<10$
No. of reflections	7138
No. of unique reflections	1823
No. of observed reflections (criterion)	1518 [$I > 3\sigma(I)$]
Absorption correction (mm^{-1}), method	6.39, empirical
R_{int}	0.048
F_{000}	318
Refinement by Jana2006 on F^2	
Parameters, constraints, restraints	131, 9, 8
R_1, wR_2 (obs)	0.0274, 0.0678
R_1, wR_2 (all)	0.0344, 0.0720
GOF (obs, all)	1.68, 1.61
Weighting scheme, weights	σ, $1/(\sigma^2(F) + 0.0004F^2)$
$\Delta\rho_{min}$, $\Delta\rho_{max}$ (e Å^{-3})	–0.58, 1.23

This is a preprint, the final version is subject to change, of the American Mineralogist (MSA)
Cite as Authors (Year) Title. American Mineralogist, in press.
DOI: https://doi.org/10.2138/am-2020-7133

Table 4. Atom coordinates and displacement parameters (Å^2) for smamite.

Atom	*x*	*y*	*z*	U_{eq}/U_{iso}	U^{11}	U^{22}	U^{33}	U^{12}	U^{13}	U^{23}
Sb[@]	0	0.5	0.5	0.01387(16)	0.0132(2)	0.0121(2)	0.0149(2)	0.00122(16)	0.00599(16)	0.00111(15)
As	0.51277(7)	0.23744(5)	0.22317(5)	0.01522(17)	0.0158(2)	0.0135(2)	0.0154(2)	0.00347(17)	0.00597(17)	0.00171(16)
Ca	0.74579(13)	0.16429(10)	0.66895(10)	0.0184(3)	0.0173(5)	0.0167(4)	0.0173(4)	0.0017(3)	0.0048(3)	0.0025(3)
O1	0.7736(4)	0.3645(4)	0.2626(4)	0.0211(12)	0.0170(16)	0.0204(15)	0.0224(16)	−0.0018(12)	0.0096(13)	0.0007(12)
OH2	0.7822(5)	0.4487(4)	0.5989(4)	0.0217(12)	0.0238(17)	0.0150(14)	0.0275(16)	0.0017(13)	0.0158(13)	−0.0011(12)
H2	0.730(7)	0.534(4)	0.648(5)	0.026*						
OH3	0.9583(5)	0.7212(4)	0.4473(4)	0.0220(12)	0.0172(16)	0.0204(15)	0.027(17)	0.0062(13)	0.0068(13)	0.0064(13)
H3	0.812(3)	0.709(6)	0.366(4)	0.0264*	0.0212(16)	0.0186(14)	0.0155(14)	−0.0006(12)	0.0054(12)	0.0051(12)
O4	0.5202(5)	0.0997(4)	0.3617(3)	0.0201(11)	0.0270(17)	0.0193(15)	0.0148(14)	0.0068(13)	0.0063(13)	−0.0010(11)
O5	0.4258(5)	0.1223(4)	0.0130(4)	0.0213(12)	0.0217(16)	0.0205(15)	0.0265(16)	0.0119(13)	0.0092(13)	0.0039(13)
O6	0.3550(5)	0.3657(3)	0.2154(4)	0.0220(12)	0.0291(18)	0.0221(16)	0.0280(17)	0.0045(14)	0.0147(14)	0.0048(13)
Ow7	0.4754(5)	0.2829(4)	0.7455(4)	0.0260(13)	0.0212(16)	0.0186(14)	0.0155(14)	−0.0006(12)	0.0054(12)	0.0051(12)
H7a	0.539(7)	0.406(2)	0.772(6)	0.0312*						
H7b	0.470(7)	0.244(6)	0.849(4)	0.0312*						
Ow8	0.9869(5)	0.9862(4)	0.7410(4)	0.0340(15)	0.030(2)	0.0296(19)	0.038(2)	0.0132(16)	0.0066(16)	0.0038(16)
H8a	1.124(5)	1.024(6)	0.844(4)	0.0408*						
H8b	0.987(8)	0.915(5)	0.638(4)	0.0408*						
Ow9	0.9350(6)	0.2801(5)	0.9757(4)	0.0413(16)	0.029(2)	0.064(2)	0.0234(19)	0.0203(19)	0.0016(15)	−0.0052(17)
H9a	1.090(3)	0.305(7)	1.049(6)	0.0496*						
H9b	0.852(7)	0.318(6)	1.038(6)	0.0496*						
H5	0.5	0	0	0.0256*						

[@] – refined occupancy 0.9376(13); * – refined with isotropic displacement parameter.

Table 5. Selected interatomic distances (Å) for smamite.

Sb–O1^{i}	2.000(2)	Ca–Oh2	2.406(3)
Sb–O1^{ii}	2.000(2)	Ca–Oh3^{v}	2.546(4)
Sb–Oh2^{i}	1.914(4)	Ca–O4	2.366(2)
Sb–Oh2^{ii}	1.914(4)	Ca–O4^{vi}	2.369(3)
Sb–Oh3^{i}	1.947(3)	Ca–Ow7	2.505(4)
Sb–Oh3^{ii}	1.947(3)	Ca–Ow8^{vii}	2.401(4)
<Sb–O>	1.95	Ca–Ow9	2.350(3)
		<Ca–O>	2.42
As–O1	1.722(3)		
As–O4	1.669(3)		
As–O5	1.697(3)		
As–O6	1.657(3)		
<As–O>	1.69		

Symmetry codes: (i) *x*–1, *y*, *z*; (ii) –*x*+1, –*y*+1, –*z*+1; (iii) *x*, *y*, *z*–1; (iv) *x*–1, *y*, *z*–1; (v) –*x*+2, –*y*+1, –*z*+1; (vi) –*x*+1, –*y*, –*z*+1; (vii) *x*, *y*–1, *z*; (viii) –*x*+2, –*y*+1, –*z*+2; (ix) –*x*+2, –*y*+2, –*z*+1; (x) –*x*+1, –*y*, –*z*; (xi) *x*–1, *y*–1, *z*–1; (xii) *x*–1, *y*–1, *z*; (xiii) *x*, *y*, *z*+1; (xiv) *x*, *y*+1, *z*; (xv) *x*+1, *y*+1, *z*+1.

Table 6. Hydrogen-bond geometry (in Å, °) in the structure of smamite.

D–H···*A*	*D*–H	H···*A*	*D*···*A*	*D*–H···*A*
Oh2–H2···O6^{ii}	0.96(5)	1.66(5)	2.586(5)	159(4)
Oh3–H3···Ow7^{ii}	0.96(2)	1.87(3)	2.807(4)	166(3)
Ow7–H7a···O6^{ii}	0.953(16)	1.792(19)	2.737(4)	171(4)
Ow7–H7b···O5^{xiii}	0.95(4)	1.81(4)	2.743(5)	167(3)
Ow8–H8a···O5^{xv}	0.97(3)	1.94(3)	2.886(4)	167(3)
Ow8–H8b···Oh3	0.97(4)	2.02(4)	2.978(5)	167(4)
Ow9–H9a···O6^{xvi}	0.97(2)	1.75(2)	2.707(4)	168(4)
Ow9–H9b···O1^{xiii}	0.97(6)	2.12(6)	3.018(5)	154(4)
O5–H5···O5^{x}	1.228(4)	1.228(4)	2.455(5)	180

Symmetry codes: (ii) –*x*+1, –*y*+1, –*z*+1; (x) –*x*+1, –*y*, –*z*; (xiii) *x*, *y*, *z*+1; (xv) *x*+1, *y*+1, *z*+1; (xvi) *x*+1, *y*, *z*+1.

This is a preprint, the final version is subject to change, of the American Mineralogist (MSA)
Cite as Authors (Year) Title. American Mineralogist, in press.
DOI: https://doi.org/10.2138/am-2020-7133

Table 8. The bond-valence analysis for smamite.*

	Sb	Ca	As	H2	H3	H5	H7a	H7b	H8a	H8b	H9a	H9b	∑BV
O1	0.80×2↓		1.13									0.06	1.99
Oh2	0.95×2↓	0.30		0.89									2.14
Oh3	0.89×2↓	0.21			0.91					0.08			2.08
O4		0.33, 0.32	1.31										1.96
O5			1.21			0.48×2↓		0.12	0.09				1.91
O6			1.36	0.18			0.13				0.14		1.81
Ow7		0.23			0.11		0.92	0.93					2.19
Ow8		0.30							0.89	0.89			2.07
Ow9		0.34									0.89	0.89	2.11
∑BV	5.28	2.02	5.02	1.07	1.01	0.97	1.05	1.05	0.98	0.96	1.03	0.95	

*All values are in valence units (*vu*); ×2↓ – multiplicity; ∑BV – sum of the bond-valences; bond–valence parameters were taken from Gagné & Hawthorne (2015) (Sb^{5+}–O, Ca^{2+}–O, As^{5+}–O) and from Brown (2002) (H^{+}–O).